Structures 87 (2026) 111724

Contents lists available at ScienceDirect

Structures

journal homepage: www.elsevier.com/locate/structures

Role of stereotomy in discontinuous modelling of masonry structures: The iconic case of the Amatrice Civic Tower

Mattia Schiavoni [a], Nuno Mendes [b], Daniel V. Oliveira [b], Gabriele Milani [c], Francesco Clementi [a,*]

[a] Department of Civil and Building Engineering, and Architecture, Polytechnic University of Marche, Ancona 60131, Italy
[b] ISISE, ARISE, Department of Civil Engineering, University of Minho, Guimarães 4800-058, Portugal
[c] Department of Architecture, Built Environment and Construction Engineering, Politecnico di Milano, Milano 20133, Italy

ARTICLE INFO

Keywords:
Masonry
Stereotomy
Failure Analysis
Distinct Element Method
Damage Evolution

ABSTRACT

The paper explores the critical role of stereotomy in the discontinuous modeling of the non-linear dynamic response of masonry structures, with a particular focus on the Amatrice Civic Tower. Situated in the Rieti province of the Lazio region, Italy, the tower has gained prominence as a symbol of resilience following the catastrophic seismic event that struck central Italy in 2016/17. The Amatrice Civic Tower is modeled using two distinct stereotomy strategies: the first represents a *realistic* configuration characterized by a chaotic texture, while the second adopts an *idealized* regularized pattern. The primary aim is to assess how these alternative stereotomies affect the resultant non-linear dynamic behavior.

Utilizing the Distinct Element Method (DEM) implemented in 3DEC©, both in-plane and out-of-plane collapses can be predicted, including potential crumbling. This approach allows for a detailed investigation of failure mechanisms and damage evolution under seismic loading. This methodological framework enables a comprehensive comparison between the numerical simulations and the actual damage sustained by the tower, thereby providing valuable insights into the role played by stereotomy in the structural resilience.

1. Introduction

Historical buildings serve as a testament to a country's cultural and artistic identity. Consequently, their preservation is a pivotal need. Over the past years, seismic events have inflicted significant losses, not only in terms of human beings, but also as far as historical and architectural estate is concerned [1–3]. In Europe, a great part of it is made by masonry [4,5]. Assessing the structural integrity of historical masonry in presence of seismic action exhibits high complexity, primarily because of the poor mechanical performance in tension of such material, which is influenced by various parameters [6,7] and that in turn is responsible for a high out-of-plane vulnerability [8]. To account for such complexity, advanced interpretative numerical models capable of accurately reproducing the mechanisms by which masonry structures respond to seismic events are needed [9,10].

In recent decades, the mechanical behavior of masonry has been investigated using a variety of approaches [11–14], each conceived to address specific aspects and differing in terms of accuracy [15,16] and applicability in standard design [17–20]. Given that masonry subjected to seismic loads requires non-linear analysis [21,22], available methods range from the simplest, such as the equivalent frame [23], to the most advanced, such as the Distinct Element Method (DEM) [24–26].

DEM models typically concentrate non-linearity at the interfaces between contiguous blocks, often assumed as rigid, whereas the Finite Element Method (FEM), traditionally regards masonry as a homogeneous continuum [27,28]. This FEM framework accelerates computations in the non-linear range and facilitates the use of constitutive laws capable of capturing softening and damage phenomena [29–32]. However, it sacrifices the detailed geometrical features of the masonry texture, limiting the ability to reproduce phenomena observed in post-earthquake surveys, such as crumbling and disaggregation of stones, as reflections of the discontinuous nature of masonry.

Significant advancements have been made in FEM-based block modelling in recent years, especially for single masonry walls, enabling a more realistic representation of texture and interfaces [33,34]. Despite these developments, application to large-scale structures remains rare,

* Corresponding author.
E-mail address: francesco.clementi@univpm.it (F. Clementi).

https://doi.org/10.1016/j.istruc.2026.111724
Received 1 November 2025; Received in revised form 15 February 2026; Accepted 22 March 2026
Available online 25 March 2026

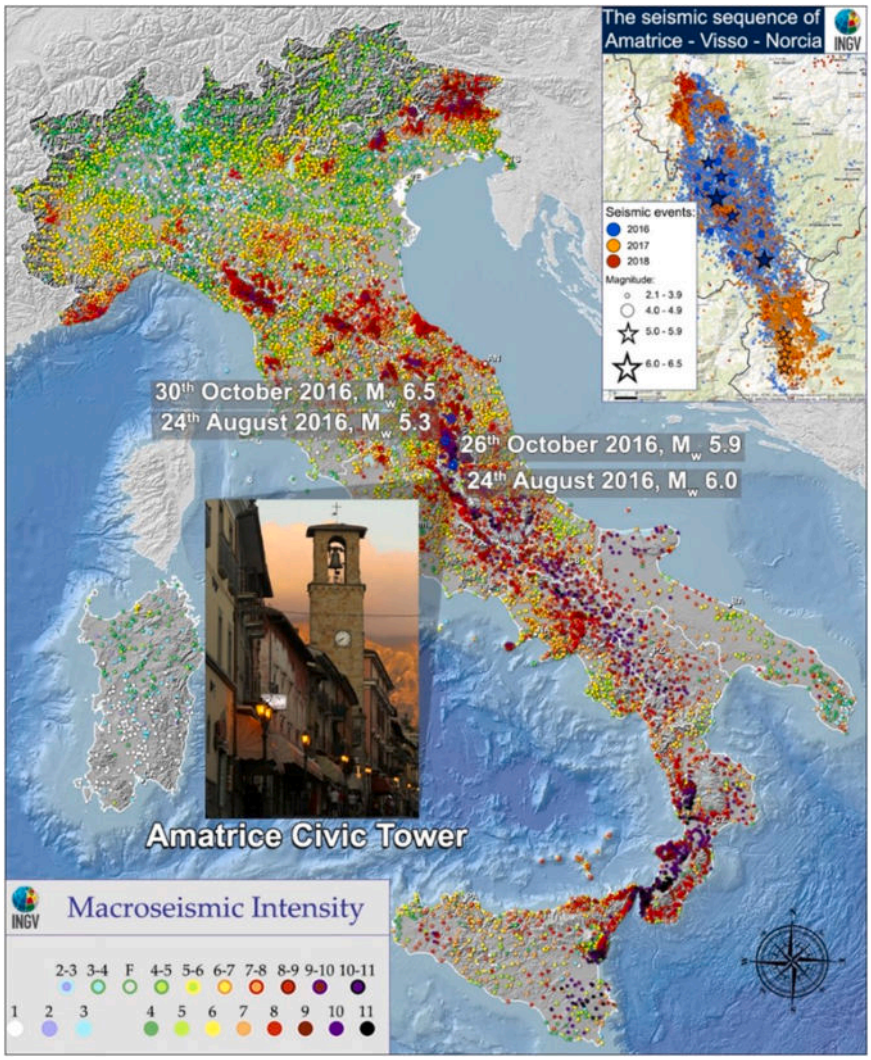

Fig. 1. Position of the Amatrice Civic Tower in Lazio Region (Italy) in the Italian Macroseismic intensity map (http://www.ingv.it/it) with the position of the seismic events.

and modelling extensive historical masonry is still a major challenge.

On the contrary, discontinuous approaches like DEM enable a more realistic prediction of localized mechanisms, particularly facilitating the identification of both in- and out-of-plane failures. Although DEM provides valuable insights, its substantial computational burden often restricts its use to specific research applications, mainly limited to small-scale examples. The constitutive behavior of joints is a key aspect that differentiates the various codes available in the literature: the Distinct Element Method (DEM) [16,35] applies smooth contact laws at block interfaces, whereas the Non-Smooth Contact Dynamic Method (NSCD) [36] adopts a non-smooth formulation for contact detection and force calculation, solving the contact problem through complementarity conditions. This allows for the simultaneous treatment of multiple persistent contacts and complex frictional interactions, which is particularly relevant in densely packed masonry systems [37,38].

A number of different studies have focused on single masonry structural elements, such as walls [39], columns, vaults, arches, or bridges [40–44]. When entire structures are considered, such as for instance towers [45–48], churches [49,50] or minarets [51], their actual geometry is typically oversimplified using large geometrically regular blocks to maintain sustainable to computational burden. Hence, it is not surprising that none of the previous studies discussed the role played by the actual stereotomy in detail. To address this knowledge gap, this paper investigates the non-linear behavior of the Civic Tower, located in the municipality of Amatrice (Rieti province, Lazio region, Italy), a symbol of resilience following the central Italy earthquakes in 2016/17. Its survival provides invaluable data on observed damage and precise geometry, offering a unique opportunity to evaluate the predictive capabilities of numerical models. The study employs the DEM to explore the influence of stereotomy, comparing two block arrangements: one highly realistic and one simplified. The objective is to assess their effectiveness in replicating the tower's actual structural response and to provide guidance on the use of numerical models that balance computational efficiency with progressive simplification.

Simulation results demonstrate that precise and detailed modeling of the arrangement and shape of the blocks are crucial for accurately determining the load-bearing capacity and, more generally, the structural behavior under seismic loads. Moreover, crumbling —a typical feature of rubble masonry that is difficult to reproduce with continuous approaches—can be reasonably captured even with a simplified stereotomy [52–54].

Finally, comparison between the results of nonlinear dynamic analyses and experimentally observed damage patterns reveals that local failures, such as those in the bell cell and the out-of-plane overturning of the external walls in the lower part, are accurately reproduced only when the stereotomy is carefully considered. Oversimplification of the block arrangement may therefore lead to misleading predictions.

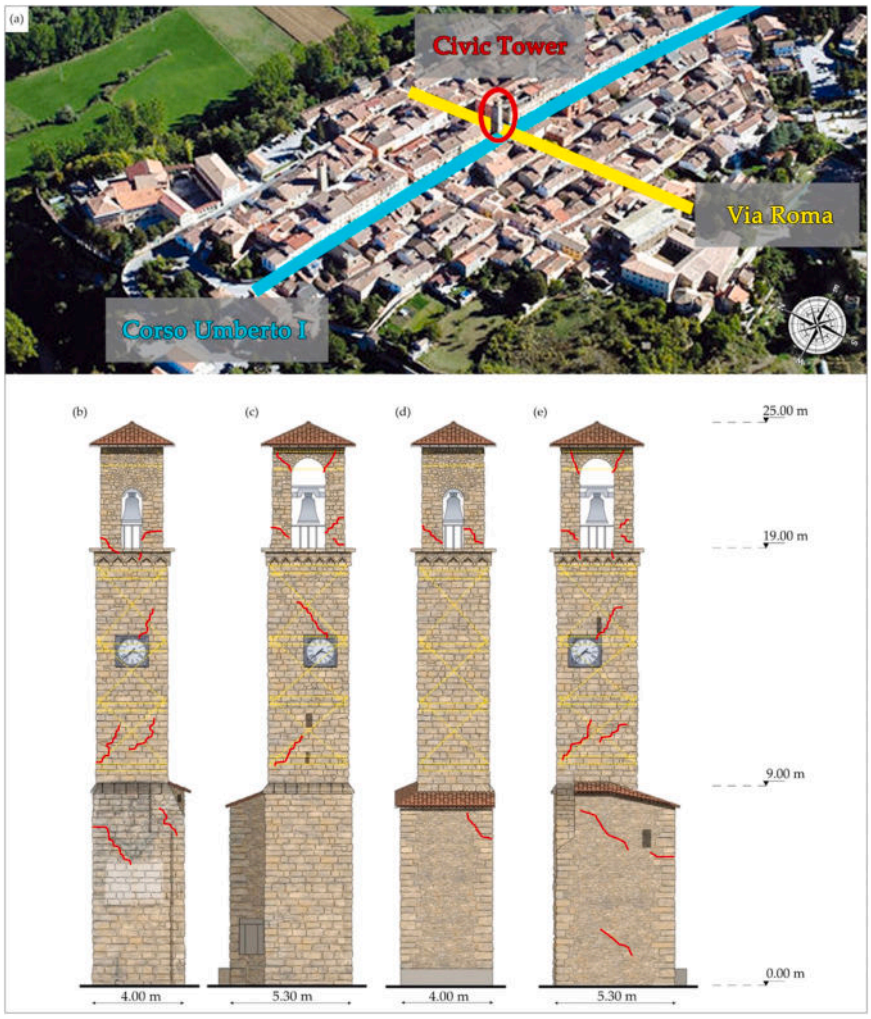

Fig. 2. – Location of the Civic tower (a) and drawing of the consolidation works carried out in the 1980: the North (b), West (c), South (d) and East (e) façade. (The yellow dashed lines represent the steel reinforcement elements).

Fig. 3. – View of the Civic Tower South (a), West (b), North (c) and East façade (d).

Fig. 4. – Damage details on the Amatrice Civic Tower after the 2016 Central Italy seismic sequence. Cracks are highlighted with black lines.

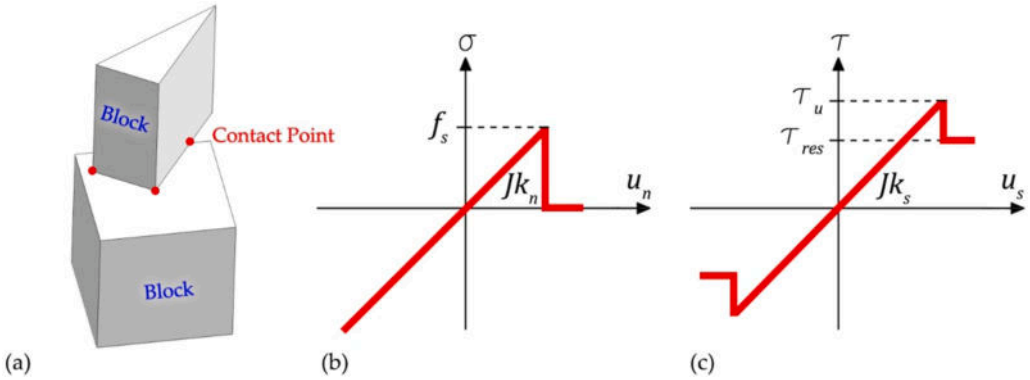

Fig. 5. – Mechanical representation of contact point between blocks (a), contact constitutive law in tension (b) and shear (c).

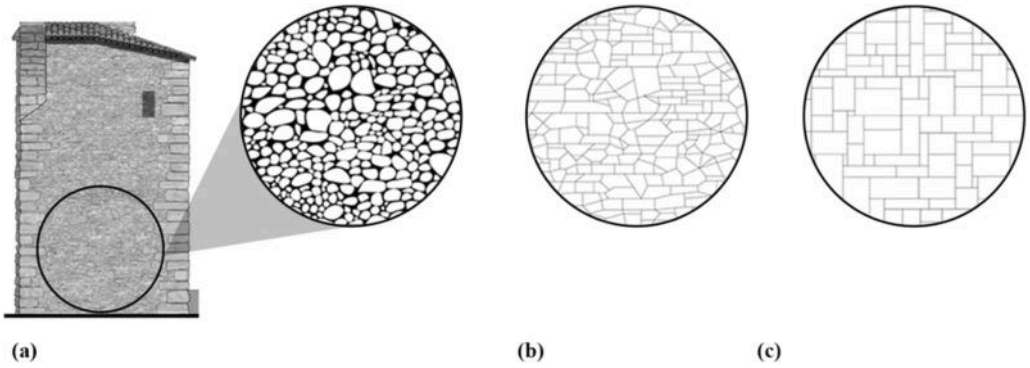

Fig. 6. –Drawing obtained from the photo-survey (a). Stereotomy realized in the realistic (a) and idealized (b) models.

2. The Amatrice Civic Tower

2.1. Historical context

Before the amost total destruction induced by the 2016/17 seismic sequence, Amatrice village (Fig. 1) was characterized by a combination of outstanding cultural landmarks and typical historic buildings. Among its most remarkable assets were noble palaces, monumental civic buildings—such as the town hall and the Civic Tower—and a multitude of churches, all testifying to the town's rich historical and artistic legacy. Alongside these prominent monuments, the historic center was largely composed by masonry buildings, generally no more than three stories high and often embellished with artistic cornices, arches, and various decorative features. The quality of masonry and the structural details throughout the town were highly heterogeneous, reflecting the diverse functions and significance of each building. Tragically, both the monumental landmarks and the more common historic dwellings suffered extensive damage or were completely destroyed during the devastating earthquakes that struck the area in 2016 and 2017 [55].

The Civic Tower stands out as one of Amatrice's most distinctive landmarks, gaining particular renown for being one of the few historic structures that did not collapse entirely following the seismic sequence, despite sustaining significant damage (Fig. 1). Located at the heart of 'Cacciatori del Tevere' square, at the intersection of Via Roma and Corso Umberto I (Fig. 2), the tower traces its origins back to medieval times, with the earliest mention in a document from 1293. Originally

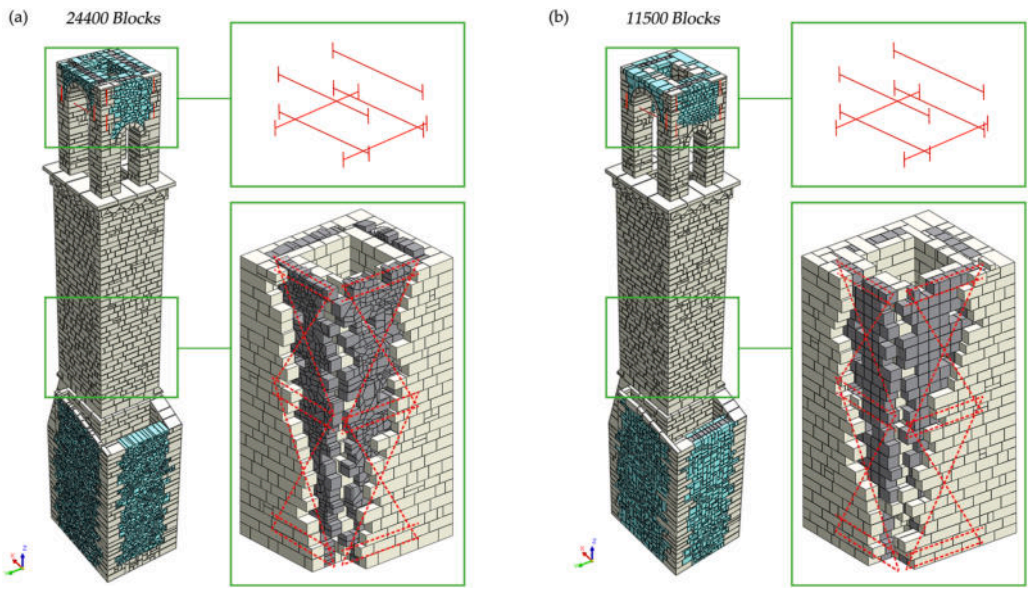

Fig. 7. – Realistic (a) and idealized (b) numerical model.

Table 1
Characteristic of the mechanical parameters used for the numerical analyses.

Parameters		Regular stones	Irregular stones	Inner rubble masonry
Density ρ	[kg/m^3]	2200	1900	1900
Joint friction μ	-	27°	27°	17°
Joint normal stiffness Jk$_n$	[Pa/m]	2.67e10	7.67e9	3.83e9
Joint shear stiffness Jk$_s$	[Pa/m]	1.07e10	3.07e9	1.53e9
Joint cohesion Jcoh	[Pa]	0.1e6	0.1e6	0.1e6
Joint tensile strength Jten	[Pa]	0.1e6	0.1e6	0.1e6

conceived as the bell tower of the Church of Santa Lucia—since the clock tower did not serve a civic function—the structure became an isolated tower in 1684 when the church was demolished by the feudal lord Alessandro Maria Orsini to widen the adjacent street. On that occasion, the base of the tower was reinforced and a small annex was added on two sides.

Throughout its existence, the tower's structural behaviour was a source of concern, particularly due to the pronounced oscillations caused by bell ringing, with some records noting maximum displacements of up to 0.20 m at the top [56]. As a result, numerous requests for intervention were documented from the 19th century onwards. Nevertheless, the only significant consolidation was undertaken between 1979 and 1985 (Fig. 2), following the Alta Valnerina earthquake, which had caused substantial damage with the formation of a deep subvertical crack. The original bell dating back to 1494 cracked in the restoration process and was replaced in 1985 with a lighter one to mitigate the excessive vibrations observed previously.

2.2. Geometry

As far as the geometry is concerned, the Civic Tower is characterized by a rectangular plan measuring 4.00 × 5.30 m, and it is approximately 25 m high (Fig. 2). At the base of the tower, there is a small annex that constitutes a projection beyond the tower walls: the east elevation with a depth of 1.50 m and the north elevation with a depth of 0.60 m. This annex hosts the staircase that allows the access from the entrance to the upper floors (Fig. 3).

Following the upward development of the section reduction, three distinct parts/blocks of the Civic Tower can be identified, characterized by different parts/blocks wall thicknesses (Fig. 2). The first floor, located at a height of around 9 m, is built with smoothed stones on the outer side and has a wall thickness that decreases by 0.15 m. The second floor marks the transition from the tower to the belfry at 19 m from the ground. The highest part of the tower includes the bell cell, which stretches the tower for additional 5 m. It is supported by four rectangular columns with cross section measuring 0.90 × 0.80 m, framing identical openings on the opposite sides. The tower is crowned by a wooden pavilion roof.

The construction material used is mainly constituted by local sandstone, which is roughly squared and arranged in a regular pattern for most of the tower, demonstrating a well-organized stereotomy from the base to the piers of the belfry. However, the masonry above the arches in the tower's upper part and annex appears to have a more disordered and incoherent stereotomy.

While the base of the tower is characterized by non-uniform wall thickness—for the wall facing Corso Umberto I (Fig. 2) and the parallel one equal to 1.15 m, for the others equal to 0.95 m— it further varies along the height of the structure. Indeed, the walls progressively become thinner with the height (from 1.00 m to 0.70 m), with a gradual reduction of 0.15 m up to the bell chamber. Notably, certain limited portions of the annex exhibit a very reduced thickness of 0.20 m.

2.3. Damage survey

In occasion of the seismic events of October 2016, the belfry of the Civic Tower—whose stability had already been compromised by the shakes occurred in August 2016—completely collapsed (Fig. 4), causing the bell detachment from its supports and the subsequent fall over the closing structure of the tower. Nevertheless, according to the report drafter by the firefighters during the tower's securing operations, no evident crack patterns or local expulsion of stone material were observed in the main core of the vertical load-bearing structure—a feature that would typically indicate significant structural distress. This finding demonstrates that the tower responded adequately to the seismic events, probably thanks to the strengthening works carried out in the 1980s, which improved the effectiveness of the connection between the orthogonal walls.

From a local perspective, the tower exhibited distinct signs of

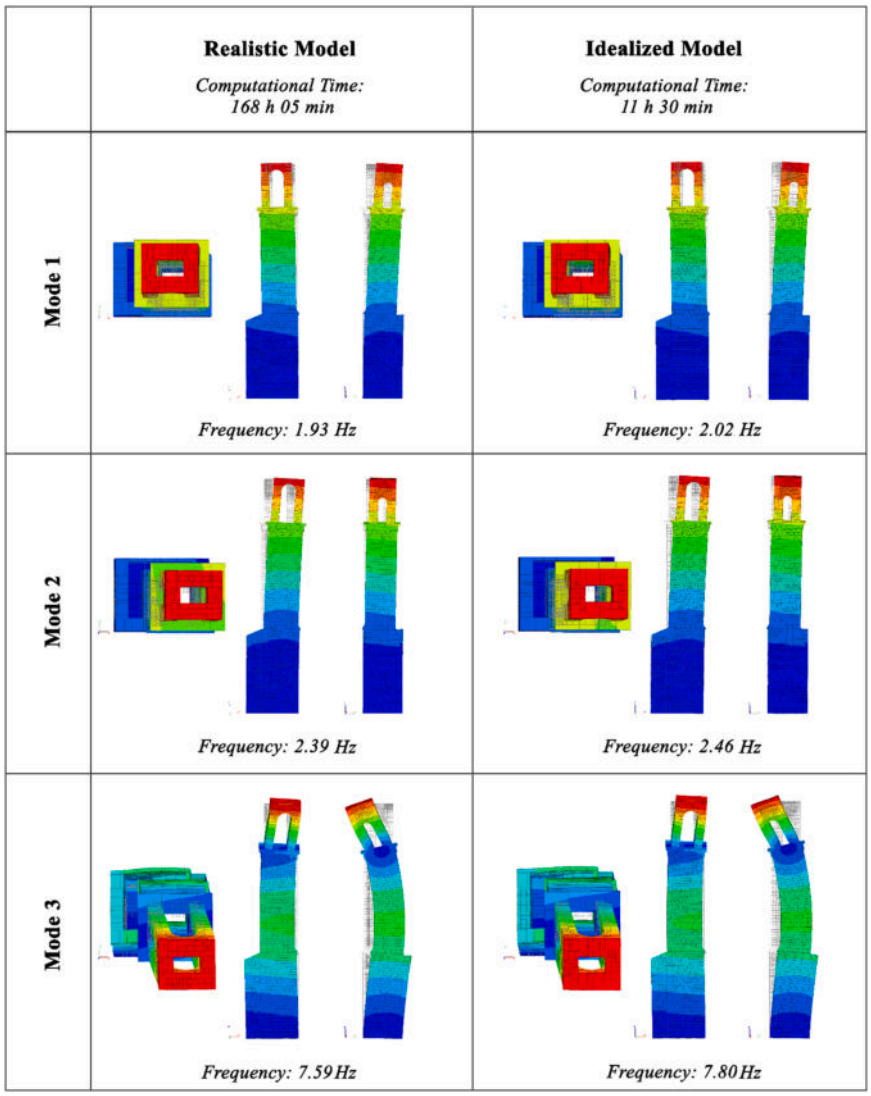

Fig. 8. – Frequencies and modes shapes of the two models.

Table 2
Characteristics of main earthquakes recorded in Amatrice (AMT) stations during the Central Italy earthquake in 2016, where * indicates that site classification is not based on direct $V_{s,30}$ measurements.

Seismic Event		M_L	Depth	Station	Class EC8	R_{jb}	R_{rup}	R_{epi}	Channel NS PGA	Channel EW PGA	Channel UD PGA
[-]		[-]	[km]	[-]	[-]	[km]	[km]	[km]	[cm/s^2]	[cm/s^2]	[cm/s^2]
1st	**24/08/2016**	6	8.1	AMT	B*	1.38	4.62	8.5	368.39	−850.8	391.37
2nd	**24/08/2016**	5.4	8	AMT	B*	-	-	20.9	−93.28	105.58	63.77
2nd	**26/10/2016**	5.9	7.5	AMT	B*	25.93	26.09	33.3	−58.55	90.74	−49.11
3rd	**30/10/2016**	6.1	9.2	AMT	B*	10.12	11.49	26.4	393.63	521.62	317.82

vulnerability, especially in the uppermost sections, where typically the inertia forces are higher. The structural response was characterized by a box-like behaviour, assumed to be generally effective. Nevertheless, the bell cell experiences significant stress due to the concentration of mass in this area, supported only by four piers. Furthermore, it is worth noting that these piers have not benefited from any structural reinforcement over the years, except for the installation of tie rods at the top of the bell chamber.

In addition, local damage was identified in the structural annex adjoining the main body of the tower (Fig. 4). This portion, built using a different construction technique and added after the construction of the tower, progressively developed significant crack patterns that required intervention to address structural weaknesses. The insufficient connection to the tower, combined with the limited wall thickness and substandard masonry quality, may explain the damage observed in reality.

3. Discontinuous approach applied to historical buildings

In the discontinuous approach, masonry is represented as an assembly of three-dimensional elements, each characterized by its own mechanical behavior and dynamic response. The interaction between elements occurs through joints, represented by points of contact. At

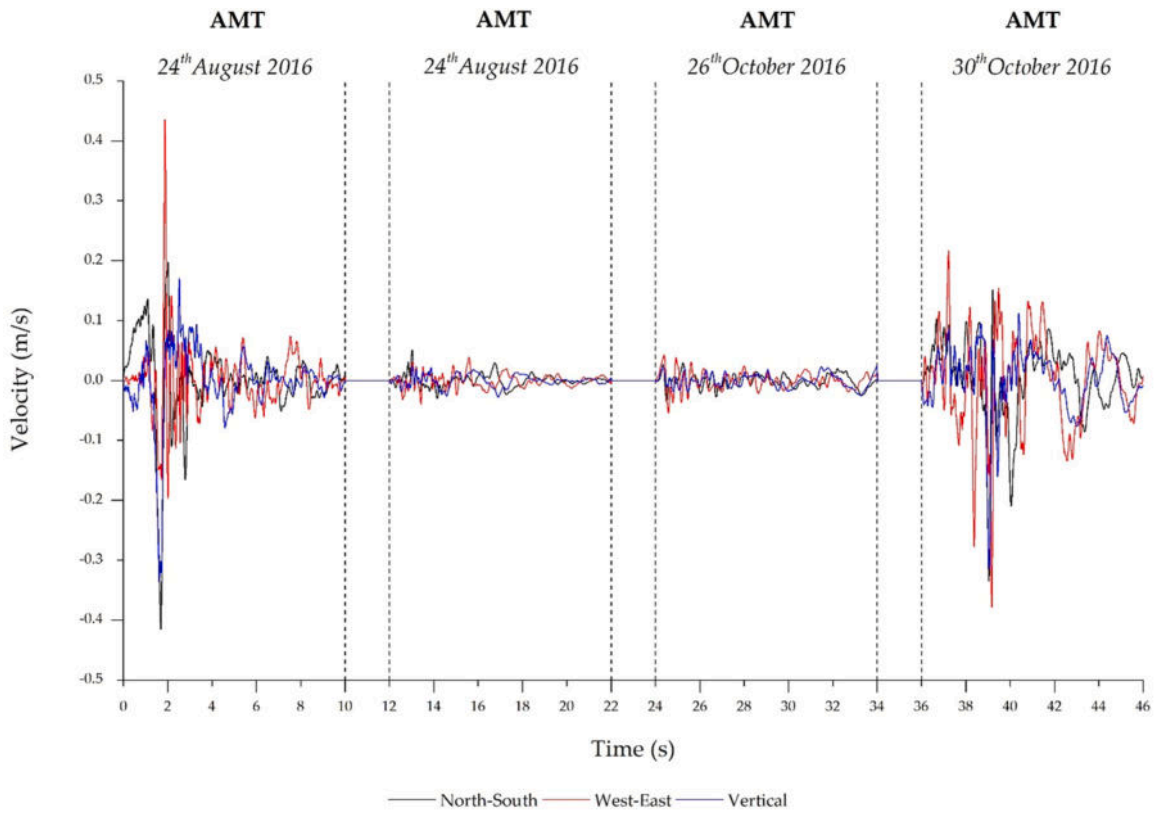

Fig. 9. –Velocity of strong motion recorded by the Amatrice (AMT) station.

these contact points, the normal and shear stress vectors are defined as functions of velocity and relative displacement. To ensure accurate results, it is necessary to use enough contact points to adequately capture the complex stress transmission and interaction mechanisms that steer the behavior of the masonry assembly under dynamic loading conditions.

DEM [57,58] is a powerful numerical approach that can capture both in-plane and out-of-plane failure mechanisms. For this reason, it was adopted for the study of the Amatrice Civic Tower. 3DEC© code was used for the numerical simulations carried out. In 3DEC©, blocks can be considered as rigid or deformable [59], but in what follows the rigid assumption is made to speed up computations without loss of accuracy.

3DEC© uses damping to boost numerical stability, as well as explicit integration schemes [60]. The sliding at the contact points is modeled using a spring-based approach ruled by linear and non-linear constitutive laws, which define the normal (Eq. 1) and shear (Eq. 2) behaviour (Fig. 5):

$$\Delta\sigma_n = JK_n\Delta_{u_n} \tag{1}$$

$$\Delta\tau_s = JK_s\Delta_{u_s} \tag{2}$$

When the peak tensile strength is reached, both cohesion and tensile strength drop to zero, while the internal friction angle remains constant. Shear sliding occurs when the applied shear stress exceeds the maximum value τ_u:

$$|\tau_s| \le c + \sigma_n \tan(\varphi) = \tau_u. \tag{3}$$

If the normal stress exceeds the tensile strength:

$$\sigma_n \le -\tau, \quad \sigma_n = 0. \tag{4}$$

Although the Mohr–Coulomb constitutive model adopted in 3DEC is widely used for its robustness and simplicity, it does not capture progressive damage, cyclic hysteresis, or stiffness degradation in compression. Recent literature has proposed advanced contact models, such as orthotropic damage-based formulations and cap models, which better represent masonry behaviour under cyclic and dynamic loading [61,62]. Despite these limitations, the Mohr–Coulomb model remains the standard for nonlinear dynamic analyses in 3DEC© due to its stability and ease of calibration.

4. Numerical models of the Amatrice Civic Tower

A refined three-dimensional discrete model was developed in MIDAS FEA NX© software to accurately reproduce the geometry of the tower, with each masonry unit represented as an individual three-dimensional solid element. Based on the actual masonry texture observed in the tower (Fig. 6a), an initial model was constructed to faithfully reproduce the pattern and arrangement of the existing joints—hereafter referred to as *realistic texture* (Fig. 6b). To evaluate the influence of stereotomy on the structural behaviour, a second model was developed, referred to as the *idealized texture (*Fig. 6c), which simplifies the geometry by using regular rectangular blocks while still aiming to maintain a joint distribution and overall texture as close as possible to the real configuration.

In both models -which are characterized in any case by a certain level of simplification-, blocks were created through convex shapes, incorporating mortar thickness into their volume. The walls were modeled considering the existence of three leaves (Fig. 7), reflecting traditional construction methods of the area for coeval buildings. This assumption was considered valid only for sufficiently thick walls, which constitute most of the tower; thinner parts, such as certain areas of the annex (only 0.20 m thick) and the four columns of the belfry, were excluded from this modelling approach.

Regarding the stereotomy, the outer leaves were reconstructed based on high-resolution photogrammetric surveys and orthophotos, which provide reliable documentation of the masonry texture. For the inner core, due to the lack of direct information, the arrangement was assumed to be chaotic in the *realistic* model (Fig. 7a), while a regularized texture was adopted for the *idealized* model (Fig. 7b). The configuration

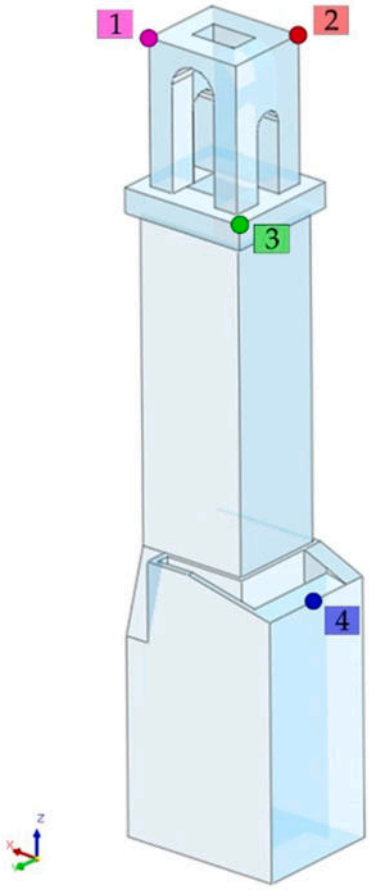

Fig. 10. – Location for the control nodes used for the nonlinear dynamic analyses of the Amatrice Civic Tower (Rieti, Italy).

of the internal portions was mainly inferred from photographic evidence contained in technical reports submitted to the local heritage authority. As a result, the *realistic* model consisted of 24400 blocks, while the *idealized* one comprised 11500 blocks.

The retrofitting interventions with steel bars along the tower and steel chains in the bell cell, carried out in the 1980s, were explicitly incorporated into both numerical models. The steel elements—including tie rods and other reinforcing bars—were modelled as solid elements with a square cross-section, assigning mechanical properties according to standard values for structural steel S235. To realistically simulate the load transfer mechanism between the steel chains at the top and the surrounding masonry, anchorage plates were also modelled at the ends of the tie rods, replicating the actual configuration (see Fig. 7, where the steel elements are highlighted in red). This modelling approach ensures that both the stiffness and the interaction effects between the reinforcement and the masonry are accurately represented in the simulations. The same strategy was consistently applied to all retrofitting rods present in the structure.

4.1. Mechanical parameters

Density value for both models was assumed with reference to typical values available in the literature for existing masonry [63]. In the impossibility to determine structural parameters through invasive material testing or dynamic identification techniques, three distinct masonry types were identified: regular stones (white blocks in Fig. 7), irregular stones (light blue blocks in Fig. 7), and internal rubble masonry (grey blocks in Fig. 7). The mechanical properties attributed to each masonry type are summarized in Table 1. The adopted mechanical parameters were defined in accordance with the Italian Building Code [64] and the related Explanatory Circular [65] for a knowledge level LC1, by applying the confidence factor CF = 1.35 to the reference mean values [66].

To ensure a realistic representation of the mechanical behavior at the interfaces between different masonry regions, the mechanical properties assigned to the joints at the boundaries (e.g., between the outer wall leaf and the internal rubble infill) were based on the characteristics of the adjacent materials. In particular, the interface between the outer and inner leaves was modeled using the mechanical parameters of the inner leaf, as this region typically governs the joint response due to its lower mechanical performance. Similarly, interfaces between the masonry blocks and the base were assigned to the properties of the base material.

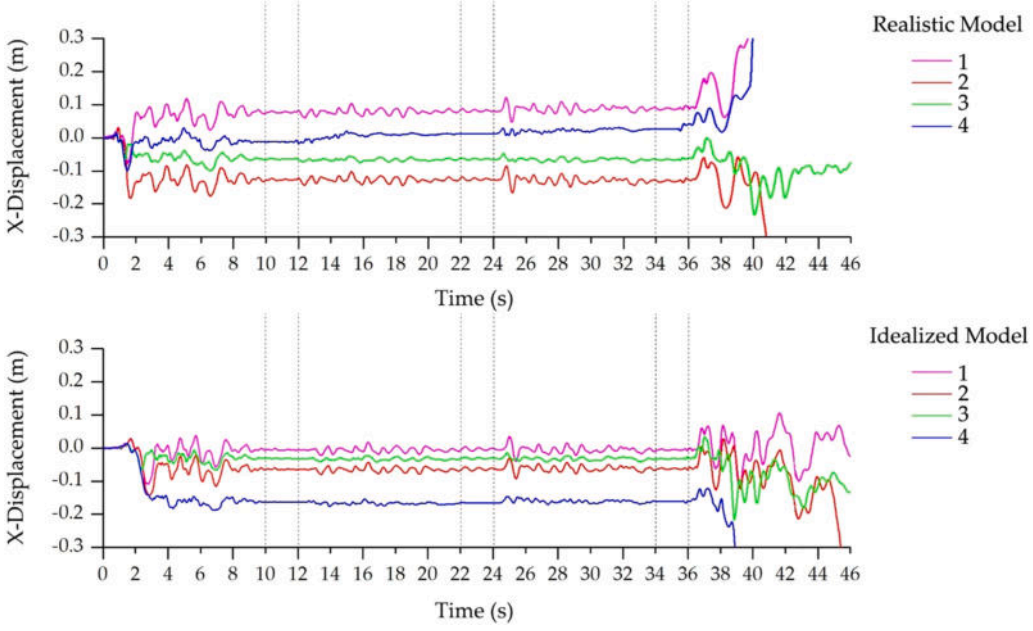

Fig. 11. – X-Displacements time histories of the Amatrice Civic Tower (Rieti province, Italy), under the four main shocks recorded in the Amatrice Station during the Central Italy seismic sequence in 2016.

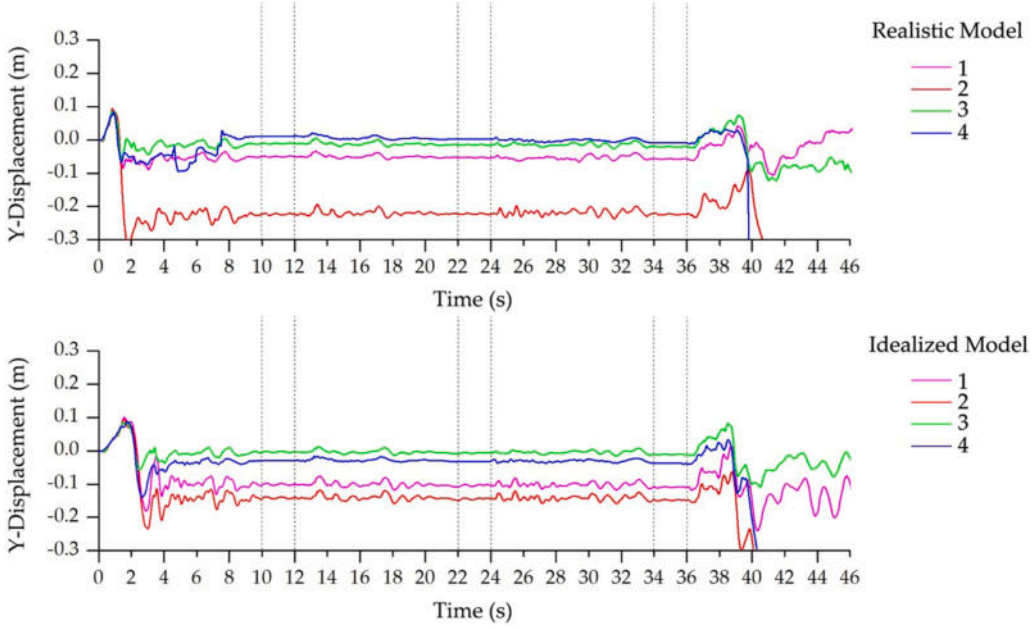

Fig. 12. – Y-Displacements time histories of the Amatrice Civic Tower (Rieti province, Italy), under the four main shocks recorded in the Amatrice Station during the Central Italy seismic sequence in 2016.

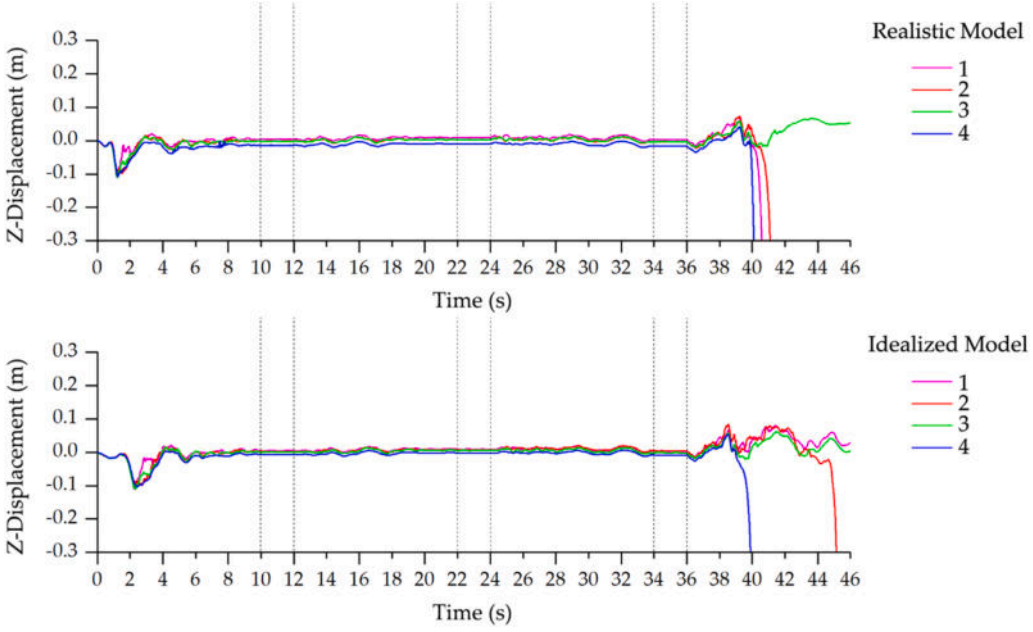

Fig. 13. – Z-Displacements time histories of the Amatrice Civic Tower (Rieti province, Italy), under the four main shocks recorded in the Amatrice Station during the Central Italy seismic sequence in 2016.

This modeling choice is supported by literature, e.g., [67–69], which indicates that the mechanical response of masonry interfaces is often dictated by the weaker or more compliant constituent. A summary of the adopted interface properties is provided in Table 1 for clarity.

4.2. Modal analysis

Linear modal analyses were performed on both the *realistic* and *idealized* numerical models to characterize the dynamic properties of the Amatrice Civic Tower. The modal analyses enabled the identification of the natural frequencies and corresponding mode shapes, and importantly, validated the mechanical parameters assigned to the contact joints as reported in Table 1. The computed frequencies and modal shapes (Fig. 8) fell within the typical ranges documented for historic masonry towers in the literature [70–73], confirming that the adopted contact parameters realistically represent the structural behavior.

Specifically, the first mode (Fig. 8) is predominantly translational, with the frequency varying from 1.93 Hz (*realistic* model) to 2.02 Hz (*idealized* model). The second mode, also mainly translational, ranges from 2.39 Hz to 2.46 Hz. The third mode is flexural, with frequencies varying from 7.59 Hz to 7.80 Hz across the two models. In all cases, the frequencies increase when transitioning from the *realistic* to the *idealized* model.

Following this validation, a global damping ratio of 3% was adopted,

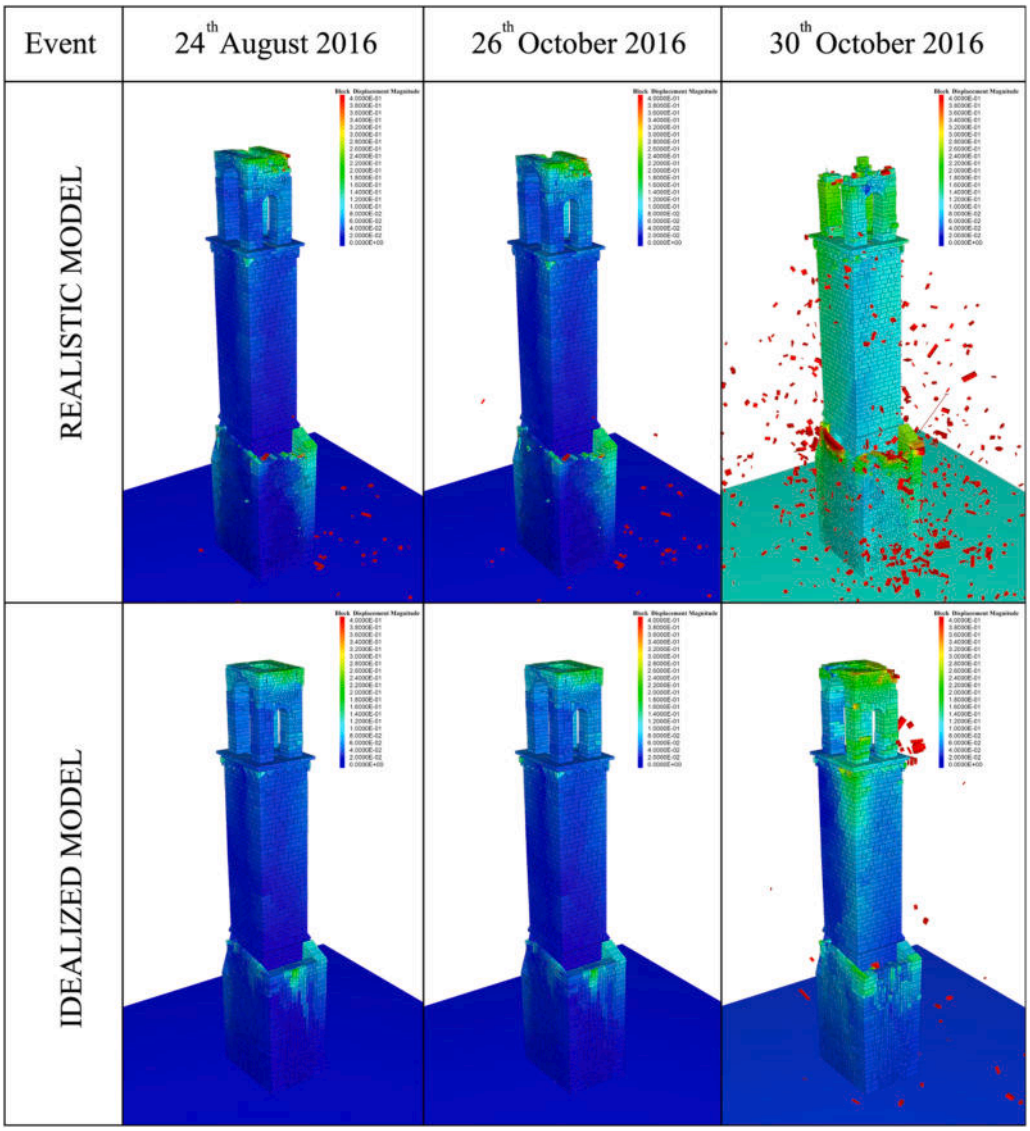

Fig. 14. Global view of the Amatrice Civic Tower showing the two numerical models under the four main seismic shocks recorded at the Amatrice station during the 2016 Central Italy seismic sequence.

in accordance with typical values reported for historic masonry structures subjected to dynamic loading [62,74] and mechanical parameters were maintained for subsequent non-linear dynamic analyses. This ensured methodological consistency and allowed for a direct comparison of the seismic response and energy dissipation characteristics between the two models.

4.3. Seismic loads

The seismic input adopted in the analyses consists of velocity records in the three principal directions (two horizontal and one vertical) acquired at the Amatrice station (AMT) during the 2016/17 Central Italy seismic sequence. The four main seismic events, summarized in Table 2, were selected to reproduce the cumulative effects of the most significant ground motions that impacted the Amatrice Civic Tower [75–77], where:

- R_{jb}, is the Joyner-Boore distance, defined as the shortest distance from the site to the surface projection of the rupture plane;
- R_{rup}, is the shortest distance between the site and the rupture surface;
- R_{epi}, is the epicentral distance, estimated by the geometric swap.

The velocity dataset (Fig. 9) spans over 46 s and was constructed by selecting 10 s of strong motion for each event, adding two seconds of rest (zero velocity) embedded between consecutive events.

The study concentrated on the four principal events, as they represent the most impactful phases of the seismic sequence. Additional shocks with magnitude greater than 5 were excluded to maintain a balance between computational efficiency and reliable results. This selection allows the dataset to capture the cumulative effects of the seismic sequence and the real process of damage accumulation, while keeping the computational demand manageable.

5. Discussion of the obtained numerical results

To compare the behavior of the two models, four strategic control nodes were identified: two at the top of the tower, one at the base of the belfry, and one in the annex (Fig. 10).

The horizontal displacement time histories recorded in correspondence of such control nodes over the entire 46-second simulation timeframe are presented in Fig. 11, Fig. 12 and Fig. 13 for both the *realistic* and *idealized* models.

A detailed analysis of the obtained results reveals clear differences in

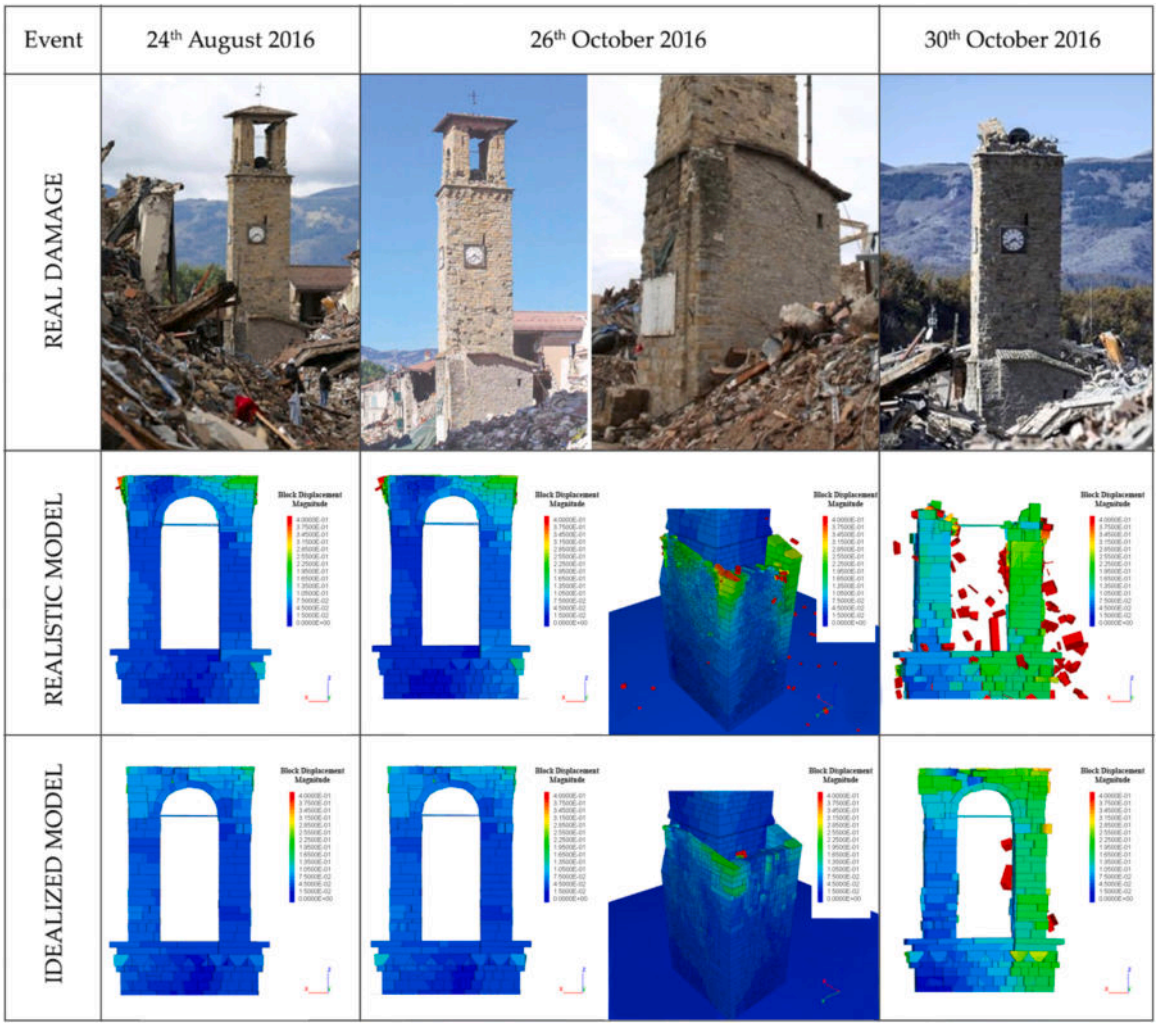

Fig. 15. – Comparison between the reality and the two numerical models of the Amatrice Civic Tower (Rieti province, Italy) under the four main shocks recorded in the Amatrice station during the Central Italy seismic sequence in 2016.

the structural response between the two models. In the *realistic* model, control node #1 collapses during the final seismic event, whereas in the *idealized* model it reaches displacements of approximately 0.20 m in the y-direction (Fig. 12) without collapsing. Similarly, control node #2 in the *realistic* model also collapses during the last event; in the *idealized* model, it reaches displacements of about 0.30 m in the y-direction, collapsing only at the very end of the seismic sequence. Conversely, control node #3 exhibits comparable displacements in both models: during the final event, this node reaches values of approximately 0.20 m in the x-direction (Fig. 11) and 0.10 m in the y-direction (Fig. 12), without collapsing. Control node #4 exhibits an analogous behavior in both models; following the first event, displacements of about 0.10 m in the y-direction and 0.20 m in the x-direction (Fig. 11) are observed, ultimately collapsing during the last event.

The results obtained show how the belfry is the most vulnerable part of the structure. Indeed, the presence of wide arched openings makes this portion particularly susceptible to damage, as illustrated in Fig. 14 and Fig. 15. Nevertheless, it is also worth noting that the presence of reinforcement interventions and an effective interconnection/interlocking between the walls prevented the activation of out-of-plane failure mechanisms in the main tower body. The annex, built in a second stage and insufficiently interconnected to the main body, is identified by the analyses carried out as the second source of specific structural vulnerability (Fig. 14 and Fig. 15).

Overall, it can be stated that the *realistic* model reproduces more faithfully the observed damage patterns, such as the collapse of the bell cell and the failures occurring in the annex. This fidelity is attributable to the detailed representation of the inner rubble masonry and stone arrangement, which is essential for capturing the collapse mechanisms. By contrast, although the *idealized* model is able to predict the development of some damage in the belfry, it underestimates the extent of the collapse observed in reality (Fig. 15). The *realistic* model, on the other hand, reproduces the collapse of the upper portion of the belfry, which is consistent with the actual damage pattern documented after the seismic sequence. While neither model predicts a complete collapse of the belfry, the *realistic* model can more accurately capture both the localization and the severity of the crumbling, offering a closer match to the post-earthquake damage survey.

To investigate the causes of the differences between the two approaches, a detailed analysis was carried out on how geometric representation may affect the seismic response. A representative 5 m x 5 m area was considered (Fig. 16), focusing on two key geometric parameters: the number of blocks and the symmetry index.

In particular, the symmetry index S is defined as the ratio between the actual perimeter of a contour and the perimeter of its convex hull:

$$S = \frac{1}{n_b}\sum_{1}^{n_b}\frac{P}{P_{conv}}, \tag{5}$$

where:

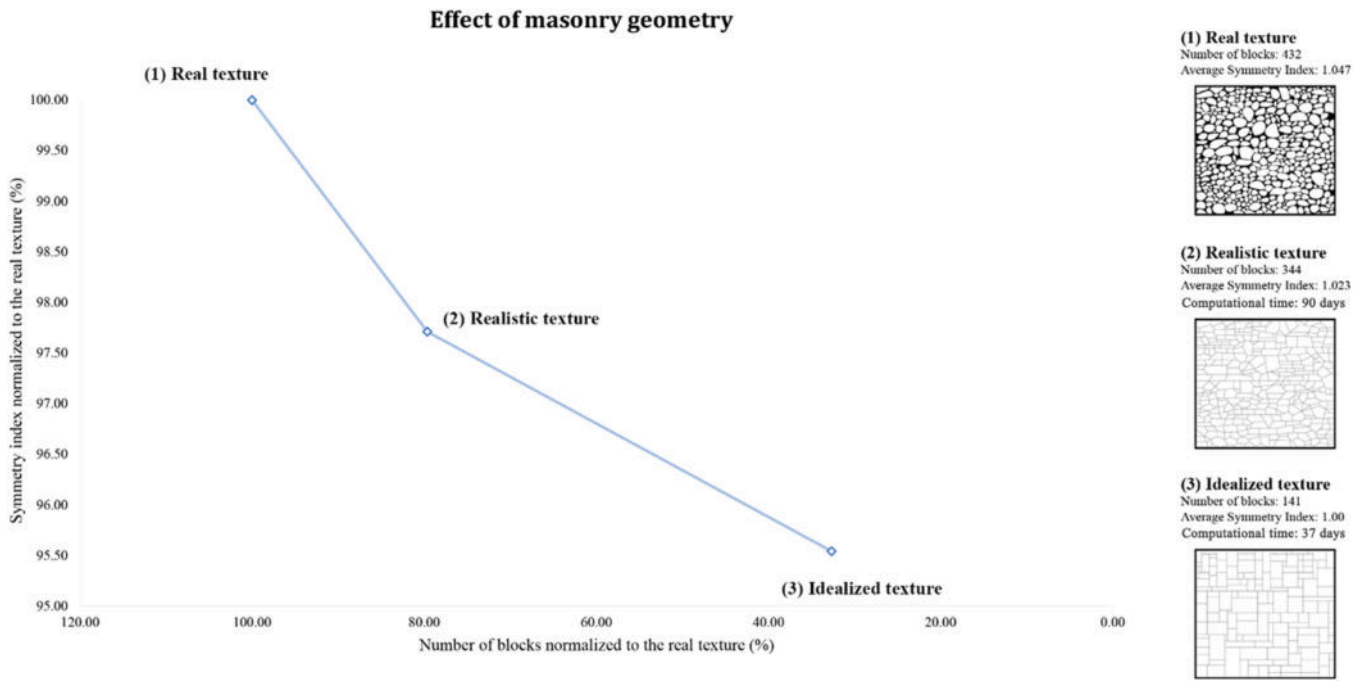

Fig. 16. – Effect of masonry geometry through block count variation and symmetry index across real, realistic, and idealized textures.

- n_b is the number of blocks;
- P is the perimeter of the actual contour;
- P_{conv} is the perimeter of the corresponding convex hull.

This index quantifies the regularity of the shapes: values close to 1 indicate perfectly regular blocks, while higher values indicate more irregular shapes.

The analysis revealed that by reducing the number of blocks by 20% and slightly increasing the symmetry index by 2.3% – both with respect to the actual masonry texture – the *realistic* model continues to reproduce the observed structural behavior with good accuracy. In this scenario, the computational burden is approximately 90 days.

In contrast, further simplifications – such as increasing the grid spacing to further reduce the number of blocks, as done in the *idealized* model – lead to a symmetry index approaching 1. This results in an unrealistic seismic response and a damage pattern that does not correspond to the observed behavior. In this case, the computational burden reduces to approximately 37 days, which represents a reduction of 53 days.

The trend shown in Fig. 16 clearly indicates that as the geometry of the blocks becomes more regular, the agreement between the numerical model and the real structural progressively decreases, at least as far as the geometry is concerned.

These findings highlight the importance of a balanced approach when modeling historic masonry structures. Highly simplified models offer reduced computation times but can produce misleading results non-representative of the expected actual behavior, while fully realistic models are highly accurate but require significant computing resources. Adopting an intermediate solution – characterized by a simplified yet still irregular masonry texture – is recommended, as it provides a good balance between computational efficiency and reliability of the results.

At this point, some limitations of the present study should be acknowledged. First, the geometric and mechanical properties of the masonry were derived from available surveys and literature data, which may not fully capture the variability and complexity of the actual materials. The stereotomy adopted in the *realistic* model is based on external photographic evidence and may not account for possible hidden heterogeneities within the wall core. Moreover, the choice of block size in the models is crucial: using blocks of a size comparable to two (or three) fused stones yields more realistic damage patterns, while larger blocks tend to oversimplify the collapse mechanisms and underestimate the role of stereotomy. The seismic input and boundary conditions are also idealized, which may affect the accuracy of the simulated response. Finally, the findings are specific to the Amatrice Civic Tower and may not be directly generalizable to other masonry structures with different geometries, stereotomies and construction techniques.

Despite the limitations pointed out above, the methodology is general and applicable to other case studies. Moreover, this study clearly demonstrates that stereotomy plays a critical role in the numerical modeling of masonry structures, significantly influencing the predicted failure mechanisms and the localization of damage. Future work should focus on improving the characterization of material properties, refining the representation of hidden masonry textures, and validating the numerical models against more comprehensive experimental or survey data.

6. Conclusion

In this paper, the role of stereotomy was investigated, and the Amatrice Civic Tower's behavior was studied using the DEM implemented in the 3DEC© code, which allows for studying both in-plane and out-of-plane behavior.

Specifically, two discontinuous models with different stereotomy were compared: in the *realistic* model, the irregularity of the stones is fully and accurately reproduced, whereas in the *idealized* model, the irregular stones are approximated as regular blocks. The contribution of previous retrofitting interventions present in the tower was also considered in both models.

To investigate these aspects, non-linear dynamic analyses were performed by applying the seismic sequence of Central Italy to both numerical models, using the ground motions recorded near the Civic Tower site. By comparing the extent of the damage in the two numerical models, it can be observed that the *idealized* model shows a greater capacity to withstand horizontal loads. On the other hand, the *realistic* model reveals vulnerabilities in the bell tower area already after the first seismic event, which progressively worsen and ultimately lead to

collapse following the last shock of the sequence. The response of the *realistic* model closely matches the actual observed behaviour: the Civic Tower suffered damage to the bell cell and adjacent structures in the early stages of the seismic sequence, ultimately culminating in the collapse of the bell tower during the final event.

Finally, the study underscores the importance of an accurate assessment during the modelling phase, as oversimplifying the stereotomy can lead to incorrect and misleading results. While simplified modelling may reduce the computational effort, it unavoidably compromises the reliability of the results obtained. Therefore, when dealing with irregular and chaotic masonry, an accurate representation of their stereotomy is essential for obtaining results that truly reflect reality.

CRediT authorship contribution statement

Mattia Schiavoni: Writing – review & editing, Writing – original draft, Software, Investigation, Formal analysis, Data curation. **Nuno Mendes:** Writing – original draft, Supervision, Software, Methodology, Investigation, Conceptualization. **Daniel V. Oliveira:** Writing – original draft, Validation, Supervision, Methodology, Investigation, Conceptualization. **Gabriele Milani:** Writing – review & editing, Writing – original draft, Supervision, Resources, Methodology, Conceptualization. **Francesco Clementi:** Writing – review & editing, Writing – original draft, Visualization, Validation, Supervision, Conceptualization.

Funding

The authors declare that no funds, grants, or other support were received during the preparation of this manuscript.

Declaration of Competing Interest

The authors declare that they have no known competing financial interests or personal relationships that could have appeared to influence the work reported in this paper.

Acknowledgement

The authors express their gratitude to Itasca Harpaceas for providing access and support for 3DEC© under the IEP program. Clementi Francesco and Mattia Schiavoni gratefully acknowledge the Italian Ministry of University (Italy) for the support under the program “Dipartimento di Eccellenza” of the Department of Civil and Building Engineering, and Architecture—Polytechnic University of Marche (Ancona, Italy).

Clementi Francesco gratefully acknowledge the WP4 line “MARS - CARTIS” of the DPC-ReLUIS 2024–2026 research project, and the Vitality project – Project Code ECS00000041, CUP I33C22001330007 - funded under the National Recovery and Resilience Plan (NRRP), Mission 4 Component 2 Investment 1.5 - 'Creation and strengthening of innovation ecosystems,' construction of 'territorial leaders in R&D′ – Innovation Ecosystems - Project 'Innovation, digitalization and sustainability for the diffused economy in Central Italy – VITALITY' Call for tender No. 3277 of 30/12/2021, and Concession Decree No. 0001057.23-06-2022 of Italian Ministry of University funded by the European Union – NextGenerationEU.

Gabriele Milani gratefully acknowledges the financial support of the Italian Ministry of Scientific Research MUR within the research project PRIN−2022 - “Advanced mechanical models and computational methods for large-scale 3Dprinting of innovative concrete structures (COMˆ3D CREATE)” (National PI: Prof. Andrea Chiozzi, Local PI: Prof. Gabriele Milani). Finanziato dall’Unione europea- Next Generation EU, Missione 4 Componente 2 CUP D53D23004070006.

Data availability

The datasets generated during and/or analyzed during the current study are available from the corresponding author on reasonable request.

References

[1] Vlachakis G, Vlachaki E, Lourenço PB. Learning from failure: damage and failure of masonry structures, after the 2017 Lesvos earthquake (Greece). Eng Fail Anal 2020;117:104803. https://doi.org/10.1016/j.engfailanal.2020.104803.
[2] Gautam D, Chaulagain H. Structural performance and associated lessons to be learned from world earthquakes in Nepal after 25 April 2015 (MW 7.8) Gorkha earthquake. Eng Fail Anal 2016;68:222–43. https://doi.org/10.1016/j.engfailanal.2016.06.002.
[3] Preciado A, Peña F, Colmenero Fonseca F, Silva C. Damage description and schematic crack propagation in Colonial Churches and old masonry buildings by the 2017 Puebla-Morelos earthquakes (Mw = 8.2 and 7.1). Eng Fail Anal 2022;141:106706. https://doi.org/10.1016/j.engfailanal.2022.106706.
[4] Onescu I, Lo Monaco A, Grillanda N, Mosoarca M, D'Amato M, Formisano A, et al. Simplified Vulnerability Assessment of Historical Churches in Banat Seismic Region, Romania. Int J Archit Herit 2024. https://doi.org/10.1080/15583058.2024.2341054.
[5] Lo Monaco A, Grillanda N, Onescu I, Fofiu M, Clementi F, D'Amato M, et al. Seismic assessment of Romanian Orthodox masonry churches in the Banat area through a multi-level analysis framework. Eng Fail Anal 2023;153. https://doi.org/10.1016/j.engfailanal.2023.107539.
[6] Lourenço PB, Mendes N, Ramos LF, Oliveira DV. Analysis of masonry structures without box behavior. Int J Archit Herit 2011;5:369–82. https://doi.org/10.1080/15583058.2010.528824.
[7] Asteris PG, Drosopoulos GA, Cavaleri L, Formisano A, Drougkas A, Milani G, et al. Mapping and revealing the nature of masonry compressive strength using computational intelligence. Structures 2025;78:109189. https://doi.org/10.1016/j.istruc.2025.109189.
[8] de Felice G, De Santis S, Lourenço PB, Mendes N. Methods and challenges for the seismic assessment of historic masonry structures. Int J Archit Herit 2016:1–18. https://doi.org/10.1080/15583058.2016.1238976.
[9] Roca P, Cervera M, Gariup G, Pela' L. Structural analysis of masonry historical constructions. classical and advanced approaches. Arch Comput Methods Eng 2010;17:299–325. https://doi.org/10.1007/s11831-010-9046-1.
[10] Penazzato L, Illampas R, Oliveira DV. The challenge of integrating seismic and energy retrofitting of buildings: an opportunity for sustainable materials? Sustainability 2024;16:3465. https://doi.org/10.3390/su16083465.
[11] Li S-Q, Zhang C, Zheng L-L, Chen P-C, Qin P-F. Comparison of vulnerability models for masonry building portfolios considering different macroseismic intensity scales. J Build Eng 2025;103:112066. https://doi.org/10.1016/j.jobe.2025.112066.
[12] Bomben L, Macorini L, Chisari C, Izzuddin BA. Mesoscale and macroscale modelling for nonlinear analysis of masonry wall structures under cyclic loading. Structures 2025;82:110209. https://doi.org/10.1016/j.istruc.2025.110209.
[13] Gouda A, ElSayed M, Salem H, Attia W, Elansary A. Applied element modelling of unreinforced and reinforced concrete masonry walls under blast loading. Structures 2023;51:828–45. https://doi.org/10.1016/j.istruc.2023.03.055.
[14] Postacchini M, Zitti G, Giordano E, Clementi F, Darvini G, Lenci S. Flood impact on masonry buildings: The effect of flow characteristics and incidence angle. J Fluids Struct 2019;88:48–70. https://doi.org/10.1016/j.jfluidstructs.2019.04.004.
[15] Kömürcü S. A comprehensive numerical study on examining the failure mechanisms of masonry walls via continuous micro modeling. Eng Fail Anal 2025;177:109680. https://doi.org/10.1016/j.engfailanal.2025.109680.
[16] Pulatsu B, Erdogmus E, Lourenço PB, Lemos JV, Tuncay K. Simulation of the in-plane structural behavior of unreinforced masonry walls and buildings using DEM. Structures 2020;27:2274–87. https://doi.org/10.1016/j.istruc.2020.08.026.
[17] Sarhosis V, Milani G, Formisano A, Fabbrocino F. Evaluation of different approaches for the estimation of the seismic vulnerability of masonry towers. Bull Earthq Eng 2018;16:1511–45. https://doi.org/10.1007/s10518-017-0258-8.
[18] Nochebuena-Mora E, Mendes N, Salvalaggio M, Lourenço PB. The seismic performance of earthen historical buildings in seismic-prone regions: the church of santo Tomás de aquino in rondocan as a complex example. Appl Sci 2025;15:7624. https://doi.org/10.3390/app15137624.
[19] Buzzetti M, Pingaro N, Milani G. Automatic detection of local collapse mechanisms in historical masonry buildings: fast and robust FE upper bound limit analysis. Eng Fail Anal 2025;170:109310. https://doi.org/10.1016/j.engfailanal.2025.109310.
[20] Szabó S, Funari MF, Casapulla C, Chryssanthopoulos M, Lourenço PB. The role of uncertainties in the seismic assessment of masonry churches affected by compound rocking failure mechanism: macro-block limit analysis investigations. Structures 2024;63:106385. https://doi.org/10.1016/j.istruc.2024.106385.
[21] Amitrano L, Di Chicco R, Formisano A. Seismic vulnerability and fragility assessment of masonry structures within the historic centre of Meta (Naples, Southern Italy). J Build Eng 2025;104:112328. https://doi.org/10.1016/j.jobe.2025.112328.
[22] Chaimae K, Younes ER, Ouadia M, Shamass R. Finite element simulation of masonry wall behavior: exploring various brick bonds and load conditions. Structures 2025;77:109089. https://doi.org/10.1016/j.istruc.2025.109089.
[23] Quagliarini E, Maracchini G, Clementi F. Uses and limits of the equivalent frame model on existing unreinforced masonry buildings for assessing their seismic risk: a review. J Build Eng 2017;10:166–82. https://doi.org/10.1016/j.jobe.2017.03.004.
[24] Giordano E, Han Y, Wang A, Bisol GD, Andrews S, Malomo D. Discontinuum rocking of rigid masonry macro-blocks using physics engines: analytical, numerical

and experimental benchmarking. Structures 2025;80:110027. https://doi.org/10.1016/j.istruc.2025.110027.
[25] Cuong NH, Luat N-V, Gayoon L, An H, Han SW, Lee K. Experimental and DEM numerical analyses of the flexural and diagonal compression behavior of masonry reinforced with polyurea coating. Structures 2023;54:1578–92. https://doi.org/10.1016/j.istruc.2023.05.051.
[26] Malomo D, Pulatsu B. Discontinuum models for the structural and seismic assessment of unreinforced masonry structures: a critical appraisal. Structures 2024;62:106108. https://doi.org/10.1016/j.istruc.2024.106108.
[27] Chen Z, Zhou Y, Kinoshita T, DeJong MJ. Distinct element modeling of the in-plane and out-of-plane response of ordinary and innovative masonry infill walls. Structures 2023;50:1447–60. https://doi.org/10.1016/j.istruc.2023.02.035.
[28] Fattahi M, Malekshahi M, Permanoon A. Mesoscale numerical modeling of unreinforced masonry wall response to underground dynamic loads: a comparative study utilizing FEM and DEM. Structures 2024;63:106460. https://doi.org/10.1016/j.istruc.2024.106460.
[29] Formisano A, Vaiano G, Fabbrocino F, Milani G. Seismic vulnerability of Italian masonry churches: the case of the nativity of blessed virgin mary in stellata of bondeno. J Build Eng 2018;20:179–200. https://doi.org/10.1016/j.jobe.2018.07.017.
[30] Valente M, Milani G. Damage assessment and collapse investigation of three historical masonry palaces under seismic actions. Eng Fail Anal 2019;98:10–37. https://doi.org/10.1016/j.engfailanal.2019.01.066.
[31] Ceroni F, Argiento LU, Casapulla C. A sensitivity study of vulnerability parameters for rocking masonry façades of single-nave churches hit by the 2016 Central Italy seismic sequence. J Build Eng 2025;108:112823. https://doi.org/10.1016/j.jobe.2025.112823.
[32] Manikandan K, Nidhi M, Micelli F, Cascardi A, Sivasubramanian MVR. Seismic vulnerability assessment of slender masonry structures: a machine learning approach with vibration-based assessment and nonlinear dynamic analysis. Structures 2025;79:109272. https://doi.org/10.1016/j.istruc.2025.109272.
[33] Ghezelbash A, Sharma S, D'Altri AM, Lourenço PB, Rots JG, Messali F. Challenges in high-fidelity implicit block-based numerical simulation of dynamic out-of-plane two-way bending in unreinforced brick masonry walls. Earthq Eng Struct Dyn 2025;54:1836–58. https://doi.org/10.1002/eqe.4337.
[34] Ghezelbash A, D'Altri AM, Sharma S, Lourenço PB, Rots JG, Messali F. A block-based numerical strategy for modeling the dynamic out-of-plane behavior of unreinforced brick masonry walls. Meccanica 2025;60:2069–105. https://doi.org/10.1007/s11012-024-01899-8.
[35] Azevedo J, Sincraian G, Lemos JV. Seismic behavior of blocky masonry structures. Earthq Spectra 2000;16:337–65. https://doi.org/10.1193/1.1586116.
[36] Chetouane B, Dubois F, Vinches M, Bohatier C. NSCD discrete element method for modelling masonry structures. Int J Numer Methods Eng 2005;64:65–94. https://doi.org/10.1002/nme.1358.
[37] Schiavoni M, Giordano E, Roscini F, Clementi F. Numerical modeling of a majestic masonry structure: a comparison of advanced techniques. Eng Fail Anal 2023;149. https://doi.org/10.1016/j.engfailanal.2023.107293.
[38] Schiavoni M, Giordano E, Roscini F, Clementi F. Numerical assessment of interacting structural units on the seismic damage: a comparative analysis with different modeling approaches. Appl Sci 2023;13. https://doi.org/10.3390/app13020972.
[39] Szabó S, Pulatsu B, Funari MF, Lourenço PB. The effect of cross-section morphology on the out-of-plane seismic behaviour of two-leaf masonry walls. J Build Eng 2025:114098. https://doi.org/10.1016/j.jobe.2025.114098.
[40] Bianchini N, Mendes N, Candeias P, Rossi M, Calderini C, Lourenço P, et al. Seismic performance of masonry cross vaults through shaking table testing on a scaled model. 12th International Conference on Structural Analysis of Historical Constructions. CIMNE; 2021. https://doi.org/10.23967/sahc.2021.230.
[41] Chen S, Ferrante A, Clementi F, Bagi K. DEM analysis of the effect of bond pattern on the load bearing capacity of barrel vaults under vertical loads. Int J Mason Res Innov 2021;6:346. https://doi.org/10.1504/IJMRI.2021.116234.
[42] Lemos J. Discrete element modeling of the seismic behavior of masonry construction. Buildings 2019;9:43. https://doi.org/10.3390/buildings9020043.
[43] Schiavoni M, Ferrante A, Salachoris GP, Mariotti C, Clementi F. Out-of-plane seismic response of a masonry facade using distinct element methods. Int J Mason Res Innov 2022;1:1. https://doi.org/10.1504/IJMRI.2022.10051745.
[44] Pingaro N, Buzzetti M, Milani G. Advanced FE nonlinear numerical modeling to predict historical masonry vaults failure: assessment of risk collapse for a long span cloister vault heavily loaded at the crown by means of a general-purpose numerical protocol. Eng Fail Anal 2025;167:109070. https://doi.org/10.1016/j.engfailanal.2024.109070.
[45] Ferrante A, Clementi F, Milani G. Advanced numerical analyses by the non-smooth contact dynamics method of an ancient masonry bell tower. Math Methods Appl Sci 2020. https://doi.org/10.1002/mma.6113.
[46] Ferrante A, Clementi F, Milani G. Dynamic behavior of an inclined existing masonry tower in Italy. Front Built Environ 2019;5:1–16. https://doi.org/10.3389/fbuil.2019.00033.
[47] Borlenghi P, Saisi A, Gentile C. Determining structural models of a masonry tower from Architectural research and operational modal analysis. J Build Eng 2025;111:113347. https://doi.org/10.1016/j.jobe.2025.113347.
[48] Mercuri M, Pathirage M, Gregori A, Cusatis G. On the collapse of the masonry Medici tower: an integrated discrete-analytical approach. Eng Struct 2021;246. https://doi.org/10.1016/j.engstruct.2021.113046.
[49] Mendes N, Zanotti S, Lemos JV. Seismic performance of historical buildings based on discrete element method: an adobe church. J Earthq Eng 2020;24:1270–89. https://doi.org/10.1080/13632469.2018.1463879.
[50] Ferrante A, Schiavoni M, Bianconi F, Milani G, Clementi F. Influence of stereotomy on discrete approaches applied to an ancient church in Muccia, Italy. J Eng Mech 2021;147:04021103. https://doi.org/10.1061/(ASCE)EM.1943-7889.0002000.
[51] Çelik A, Kocaman İ, Mercimek Ö, Anıl Ö, Fener M, Çelik B, et al. Understanding roots of failure of historical Ottoman monumental buildings by means of advanced finite element modelling: the effect of the 1939 Erzincan earthquake on Nafiz Pasha Bath-house and Izzet Pasha Mosque. Eng Fail Anal 2025;179:109811. https://doi.org/10.1016/j.engfailanal.2025.109811.
[52] Schiavoni M, Giordano E, Roscini F, Clementi F. Advanced numerical insights for an effective seismic assessment of historical masonry aggregates. Eng Struct 2023;285:115997. https://doi.org/10.1016/j.engstruct.2023.115997.
[53] Schiavoni M, Di Giosaffatte M, Roscini F, Clementi F. Mechanisms detection by nonlinear finite and distinct element simulations of a historical religious masonry complex. Bull Earthq Eng 2025. https://doi.org/10.1007/s10518-025-02125-w.
[54] Schiavoni M, Roscini F, Clementi F. Comparative analysis between continuous and discontinuous methods for the assessment of a cultural heritage structure. Meccanica 2025;60:1957–82. https://doi.org/10.1007/s11012-024-01885-0.
[55] Fiorentino G, Forte A, Pagano E, Sabetta F, Baggio C, Lavorato D, et al. Damage patterns in the town of Amatrice after August 24th 2016 Central Italy earthquakes. Bull Earthq Eng 2018;16:1399–423. https://doi.org/10.1007/s10518-017-0254-z.
[56] Jain A, Acito M, Chesi C, Magrinelli E. The seismic sequence of 2016–2017 in Central Italy: a numerical insight on the survival of the Civic Tower in Amatrice. Bull Earthq Eng 2020;18:1371–400. https://doi.org/10.1007/s10518-019-00750-w.
[57] Cundall P.A. A computer model for simulating progressive large-scale movements in blocky rock systems. Proocedings of the Symposio of the International Society of Rock Mechanics, Nancy 2, 1971.
[58] Cundall PA, Strack ODL. A discrete numerical model for granular assemblies. Géotechnique 1979;29:47–65. https://doi.org/10.1680/geot.1979.29.1.47.
[59] Lemos JV. Discrete Element Modeling of Masonry Structures. Int J Archit Herit 2007;1:190–213. https://doi.org/10.1080/15583050601176868.
[60] Sarhosis V, Lemos JV, Bagi K. Discrete element modeling. Numer Model Mason Hist Struct 2019:469–501. https://doi.org/10.1016/B978-0-08-102439-3.00013-0.
[61] Teschemacher T, Kalkbrenner P, Pelà L, Wüchner R, Bletzinger K-U. An orthotropic damage model for masonry walls with consistent damage evolution laws. Mater Struct 2023;56:151. https://doi.org/10.1617/s11527-023-02220-x.
[62] Oktiovan YP, Messali F, Pulatsu B, Sharma S, Lemos JV, Rots JG. Cyclic constitutive model for masonry joint damage and energy dissipation using the distinct element method. Comput Struct 2026;321. https://doi.org/10.1016/j.compstruc.2025.108094.
[63] Milani G. Vulnerability evaluation of historical masonry structures: Italian Churches and Towers. RILEM Book 2019;18:19–32. https://doi.org/10.1007/978-3-319-99441-3_2.
[64] Ministero delle Infrastrutture e dei Trasporti. Aggiornamento delle "Norme Tec per Le Costr" - NTC 2018 (Ital) 2018:1–198.
[65] Ministero delle Infrastrutture e dei Trasporti. Circ 21 gennaio 2019 N 7C S Ll Pp Istruzioni per l'Appl dell'«Aggiornamento delle "Norme Tec per Le Costr"» di cui al Decret Minist 17 gennaio 2018 (19A00855) (GU Ser Gen N 35 Del 11-02-2019 - Suppl Ordin N 5) (Ital) 2019:1–300.
[66] Standoli G, Di Giosaffatte M, Schiavoni M, Roscini F, Clementi F. Sustainable structural health assessment of heritage masonry towers using artificial intelligence and data-driven monitoring: insights from the civic tower of Matelica. Eng Appl Artif Intell 2026;163:113097. https://doi.org/10.1016/j.engappai.2025.113097.
[67] Azevedo J, Sincraian G, Lemos JV. Seismic behavior of blocky masonry structures. Earthq Spectra 2000;16:337–65. https://doi.org/10.1193/1.1586116.
[68] Sarhosis V, Lemos JV. A detailed micro-modelling approach for the structural analysis of masonry assemblages. Comput Struct 2018;206:66–81. https://doi.org/10.1016/j.compstruc.2018.06.003.
[69] Ferrante A, Loverdos D, Clementi F, Milani G, Formisano A, Lenci S, et al. Discontinuous approaches for nonlinear dynamic analyses of an ancient masonry tower. Eng Struct 2021;230. https://doi.org/10.1016/j.engstruct.2020.111626.
[70] Gentile C, Saisi A. Ambient vibration testing of historic masonry towers for structural identification and damage assessment. Constr Build Mater 2007;21:1311–21. https://doi.org/10.1016/j.conbuildmat.2006.01.007.
[71] Gentile C, Saisi A, Cabboi A. Structural identification of a masonry tower based on operational modal analysis. Int J Archit Herit 2015;9:98–110. https://doi.org/10.1080/15583058.2014.951792.
[72] Masciotta M.G., Standoli G., Giordano E., Clementi F., Oliveira D.V., Lourenço P.B. The Key Role of Structural Health Monitoring as a Control Tool in the Post-earthquake Recovery Phase of Damaged Heritage Buildings: The Case Study of "Collegiata di Santa Maria" in Visso, Italy, 2025, p. 21–45. https://doi.org/10.1007/978-3-031-93753-8_2.
[73] Monchetti S, Bartoli G, Betti M, Casolo S, Clementi F. Refining the masonry shear modulus in masonry towers via Bayesian model updating. Probabilistic Eng Mech 2026:103903. https://doi.org/10.1016/j.probengmech.2026.103903.
[74] Lemos JV, Sarhosis V. Dynamic analysis of masonry arches using Maxwell damping. Structures 2023;49:583–92. https://doi.org/10.1016/j.istruc.2023.01.139.

[75] Pacor F, Paolucci R, Luzi L, Sabetta F, Spinelli A, Gorini A, et al. Overview of the Italian strong motion database ITACA 1.0. Bull Earthq Eng 2011;9:1723–39. https://doi.org/10.1007/s10518-011-9327-6.
[76] Luzi L., Pacor F., Puglia R. Italian Accelerometric Archive v 2.3. Rome: 2017. https://doi.org/10.13127/ITACA.2.3.
[77] Pierdicca A, Clementi F, Maracci D, Isidori D, Lenci S. Damage detection in a precast structure subjected to an earthquake: a numerical approach. Eng Struct 2016;127:447–58. https://doi.org/10.1016/j.engstruct.2016.08.058.